Asian Journal of Chemistry; Vol. 37, No. 5 (2025), 1191-1196

ASIAN JOURNAL OF CHEMISTRY

https://doi.org/10.14233/ajchem.2025.33652

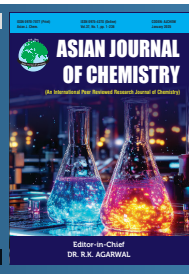

Zinc(II) Complexes Containing Aromatic Hydrazones: Synthesis, Spectral Characterization, Luminescent Properties and α-Glucosidase Inhibition

QUANG TRUNG NGUYEN* and PHUONG NAM PHAM THI

Institute of Chemistry, Vietnam Academy of Science and Technology, 18 Hoang Quoc Viet Str., Cau Giay Dist., Hanoi, Vietnam

*Corresponding author: E-mail: nqtrung@ich.vast.vn

Received: 9 March 2025; *Accepted*: 14 April 2025; *Published online*: 30 April 2025; AJC-21987

Four zinc(II) complexes were synthesized by the coordinating Zn^{2+} ions with novel aromatic hydrazone ligands. Based on the spectral analyses, the molecular ratio of Zn(II) ions to hydrazone ligands was established as 1:2, and a tetrahedral geometry around the zinc metal center was proposed for the synthesized aromatic hydrazone zinc(II) complexes. The aromatic hydrazone ligands probably coordinated with the metal Zn^{2+} *via* the carbonyl oxygen and deprotonated oxygen of salicyl ring. The fluorescence spectra of the synthesized zinc(II) complexes were analyzed in dichloromethane, revealing that the aromatic hydrazone ligands with various substituents generated a blue shift in the maximum emissions of the corresponding zinc(II) complexes. The inhibition of α-glucosidase by the synthesized hydrazone compounds was evaluated, and based on the antidiabetic activity results, the synthesized zinc(II) complexes demonstrate superior efficacy compared to the corresponding aromatic hydrazone ligands.

Keywords: Aromatic hydrazones, Zinc(II) complexes, Spectral characterization, Luminescent properties, α-Glucosidase inhibition.

INTRODUCTION

Hydrazones are considered as interesting organic molecules with great attention from both academic and industrial chemists for last few decades due to their possible synthesis, flexible structures and numerous coordination capability [1-3]. They can play as polydentate ligands which can chelate with a diversity of metal ions, both transition and non-transition metals, to form stable metal complexes [4,5]. The binding modes of hydrazones and geometry of metal complexes depend on both the metal ion and the structure of hydrazones. Besides their interesting applications in catalysis [6-10], sensors [11-14] and materials science [15-17], hydrazones had exhibited significant bioactivities such as antimicrobial, enzyme inhibition, antiviral, antioxidant, antihypertensive, anti-tubercular, anti-inflammatory and anticancer activities [18-25]. As aromatic hydrazones contains nucleophilic nitrogen atoms and the carbon atom has both nucleophilic and electrophilic effect [16,26], they have flexible ligands in the coordination chemistry [27,28]. These hydrazone especially in Schiff base containing ONO donor atoms can react with metal ions in the ketonic and enolic form to induce various metal complexes [29,30].

The long-term high levels of blood glucose in patients with diabetes mellitus induce various disorders of small blood vessels and are the reason of serious nerve, heart, kidney, eye diseases and obesity [31,32]. At present, type 2 diabetes mellitus has emerged as a global public health concern that has garnered significant attention from researchers worldwide [33]. Several remedies were proposed to address this issue, including novel oral drugs derived from organic compounds [34]. However, some medicines cause unwanted side effects. Recently, treatment of diabetes mellitus by oral α-glucosidase inhibitors has harvested much progress including potent zinc(II) complexes with various organic ligands [35-38]. The study on structure-activity relationship of the zinc(II) complexes indicated that the coordination mode and bioavailability effect their therapeutic potency. The nature and geometry of hydrazone based ligands can also play a crucial role in their bioactivity [39,40]. However, nowadays more efforts are still needed to get a high efficient drug. Herein, in this work, few zinc(II) complexes with some aromatic hydrazones are synthesized and characterized. Furthermore, *in vitro* α-glucosidase inhibition of these synthesized compounds are also examined for their antidiabetic activity.

EXPERIMENTAL

The chemicals and reagents used were of analytically pure and purchased from Across Organics Chemical company. Organic solvents such as methanol, ethanol, DMSO, chloroform were supplied by Chinese Xilong Chemical company and purified following laboratory procedures before using. The NMR spectra were recorded on a Bruker Advance NEO spectrometer with 600 MHz for ^{1}H NMR and 150 MHz for ^{13}C NMR using DMSO-d_6 as the solvent and TMS as an internal reference. Electrospray ionization mass spectra (*m/z*) were estimated using an Agilent 6310 Ion Trap spectrometer as ESI-MS. A Sciex X500 QTOF spectrometer was utilized for high-resolution mass spectrometry (HRMS) analysis. The FT-IR spectra of 4000–400 cm^{-1} were determined by a Perkin-Elmer Spectrum-2 spectrophotometer spectra using KBr pellets. Absorption spectra were recorded on a Perkin-Elmer Lambda UV-35 spectrophotometer in the range of 200-800 nm using methanol as solvent.

Synthesis of aromatic hydrazone ligands: The aromatic hydrazones were synthesized by following the reported procedures [41-43]. In brief, corresponding aromatic aldehydes (3.0 mmol) dissolved in 15 mL ethanol was added slowly to 3.0 mmol 4-hydroxy-benzohydrazide or isonicotinohydrazide dissolved in 20 mL ethanol. The reaction mixture was stirred at room temperature for about 4 h and the progress of reaction was monitored by TLC in hexane:ethylacetate (1:1). The obtained white precipitates were filtered, washed with cold ethanol, dried under low pressure and finally recrystallized in ethyl acetate (**Scheme-I**). The ligands are soluble in polar organic solvents such as DMSO, methanol, ethylacetate, dichloromethane, *etc*.

(*E*)-4-hydroxy-*N*′-(2-hydroxybenzylidene)benzohydrazide (BHB): White powder, yield: 86.5%; HRMS (*m/z*): 257.0915 $[M+H]^+$ (calcd. 257.0921); FT-IR (KBr, ν_{max}, cm^{-1}): 3319 (O–H), 3150 (N–H), 3081 (C–H), 1639 (C=O), 1607 (C=N), 1540 (C=C), 1487, 1278 (C–O), 1235, 1173, 1158 (N–N), 843, 745, 730 (C–H); ^{1}H NMR (500 MHz, DMSO-d_6, δ ppm): 11.91 (s, 1H, NH), 11.42 (s, 1H, OH), 10.16 (s, 1H, OH), 8.60 (s,1H, CH=N), 7.84 (d, *J* = 7.0, 2H–Bz), 7.51 (dd, *J* = 6.5, 1.0, 1H–Sal), 7.30 (dt, *J* = 7.0, 1.0, 1H–Sal), 6.92-6.94 (m, 2H–Sal), 6.88 (dd, *J* = 6.0, 1.5, 2H-Bz); ^{13}C NMR (125 MHz, DMSO-d_6, δ ppm): 162.40 (1C, C=O), 160.86 (1C, C–O), 157.40 (1C, C–O), 147.62 (1C, C=N), 131.08 (1C–Sal), 129.66(1C–Sal), 129.60 (1C, C–Bz), 123.17 (1C, C–Sal), 119.23 (2C, 2C–Bz), 118.65 (1C, C–Sal), 116.35 (1C, C–Sal), 115.07 (2C, C–Bz). UV-Vis [MeOH, 5.0 × 10^{-5} M, λ (nm), ε (cm^{-1} M^{-1})]: 222 (12,000), 290 (17,500), 301 (19,700), 328 (12,900).

(*E*)-*N*′-(5-Chloro-2-hydroxybenzylidene)-4-hydroxybenzohydrazide (CBHB): White powder, yield: 84.5%; ESI-MS (*m/z*): 290.8 $[M+H]^+$ (calcd. 291.7); FT-IR (KBr, ν_{max}, cm^{-1}): 3231 (d, O–H and N–H), 3024 (C–H), 1616 (C=O), 1605 (C=N), 1544 (C=C), 1475, 1341, 1267 (C–O), 1211, 1171, 1106 (N–N), 848, 767 (C–H), 700, 646, 615, 477 (C–Cl); ^{1}H NMR (500 MHz, DMSO-d_6, δ ppm): 11.99 (s, 1H, NH), 11.41 (s, 1H, OH), 10.17 (s, 1H, OH), 8.58 (s,1H, CH=N), 7.84 (d, *J* = 7.0, 2H–Bz), 7.64 (s, 1H–Sal), 7.30 (dd, *J* = 7.0, 2.0, 1H–Sal), 6.95 (d, *J* = 7.0, 1H–Sal), 6.88 (d, *J* = 7.5, 2H-Bz); ^{13}C NMR (125 MHz, DMSO-d_6, δ ppm): 162.54 (1C, C=O), 160.94 (1C, C–O), 155.98 (1C, C–O), 145.23 (1C, C=N), 130.47 (1C–Sal), 129.75 (1C, C–Bz), 127.79 (1C, C–Sal), 123.09 (1C, C–Sal), 122.87 (1C, C–Cl), 120.66 (1C, C–Sal), 118.17 (2C, 2C–Bz), 115.08 (2C, C–Bz). UV-Vis [MeOH, 5.0 × 10^{-5} M, λ (nm), ε (cm^{-1} M^{-1})]: 224 (13,600), 292 (18,100), 303 (18,900), 340 (9,800).

(*E*)-4-Hydroxy-*N*′-(2-hydroxy-3-methoxybenzylidene)-benzohydrazide (MBHB): White powder, yield: 65.5%; HRMS (*m/z*): 287.1019 $[M+H]^+$ (calcd. 287.1026); FT-IR (KBr, ν_{max}, cm^{-1}): 3446 (O–H), 3196 (N–H), 3012 (C–H), 1644 (C=O), 1605 (C=N), 1576 (C=C), 1465, 1367, 1277 (C–O), 1246, 1185, 1079 (N–N), 837, 729, 618, 481 (C–H); ^{1}H NMR (500 MHz, DMSO-d_6, δ ppm): 11.87 (s, 1H, NH), 11.14 (s, 1H, OH), 10.18

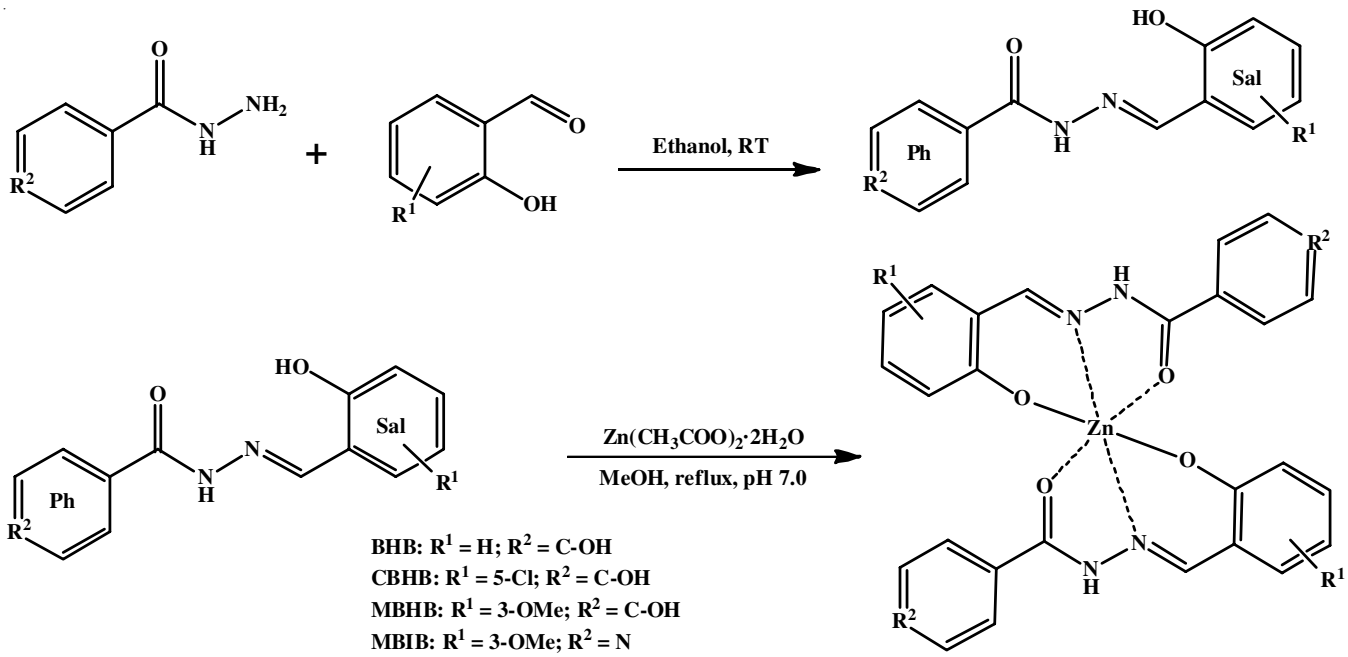

Scheme-I: Synthesis of aromatic hydrazones and their zinc(II) complexes

(s, 1H, OH), 8.60 (s,1H, CH=N), 7.82 (d, *J* = 7.0, 2H–Bz), 7.10 (d, *J* = 6.5, 1H–Sal), 7.02 (d, *J* = 6.0, 1H–Sal), 6.87 (d, *J* = 7.0, 2H-Bz), 6.86 (t, *J* = 6.5, 1H–Sal), 3.81 (s, 3H–OMe); ^{13}C NMR (125 MHz, DMSO-d_6, δ ppm): 162.46 (1C, C=O), 160.89 (1C, C–O), 147.94 (1C, C–O), 147.59 (1C, C–O), 147.17 (1C, C=N), 129.72 (2C, C–Bz), 123.25 (1C–Sal), 121.05 (1C–Sal), 119.00 (1C, C–Sal), 118.82 (1C, C–Bz), 115.13 (2C, C–Bz), 113.79 (1C, C–Sal), 55.86 (1C, OCH_3). UV-Vis [MeOH, 5.0×10^{-5} M, λ (nm), ε (cm^{-1} M^{-1})]: 225 (13,900), 304 (18,900).

(*E*)-*N*′-(2-Hydroxy-3-methoxybenzylidene)isonicotinohydrazide (MBIB): White powder, yield: 68.0%; HRMS (*m/z*): 272.1019 $[M+H]^+$ (calcd. 272.1030); FT-IR (KBr, ν_{max}, cm^{-1}): 3202 (d, O–H and N–H), 3064 (C–H), 1688 (C=O), 1603 (C=N), 1564 (C=C), 1464, 1413, 1286 (C–O), 1245, 1157, 1066 (N–N), 973, 837, 740, 651, 458 (C–H); ^{1}H NMR (500 MHz, DMSO-d_6, δ ppm): 12.25 (s, 1H, NH), 10.71 (s, 1H, OH), 8.71 (s,1H, CH=N), 8.79 (dd, *J* = 8.5;1.5, 2H–Bz), 7.85 (dd, *J* = 8.5; 1.5, 2H–Bz), 7.20 (dd, *J* = 7.0, 1.5, 1H–Sal), 7.04 (dd, *J* = 6.5, 1.5, 1H–Sal), 6.87 (t, *J* = 6.5, 1H–Sal), 3.82 (s, 3H–OMe); ^{13}C NMR (125 MHz, DMSO-d_6, δ ppm): 161.27 (1C, C=O), 150.33 (2C, C=N–C), 148.85 (1C, C–O), 147.95 (1C, C–O), 147.17 1C, C=N), 139.98 (1C, C–Bz), 128.45 (2C, C–Bz), 120.44 (2C, C–Sal), 119.08 (1C–Sal), 118.94 (1C, C–Sal), 113.89 (1C, C–Sal), 55.82 (1C, OCH_3). UV-Vis [MeOH, 5.0×10^{-5} M, λ (nm), ε (cm^{-1} M^{-1})]: 225 (15,200), 310 (12,600), 393 (4,200).

Synthesis of zinc(II) complexes: The aromatic hydrazone zinc(II) complexes were synthesized using the known modified procedures [44,45]. The solution of $Zn(CH_3COO)_2{\cdot}2H_2O$ (1.0 mmol) dissolved in 15 mL methanol was added slowly into the solution of 2.0 mmol respective aromatic hydrazone ligands (**BHB**, **CBHB**, **MBHB** or **MBIB**) dissolved in 20 mL methanol. The reaction mixture was refluxed for 3 h and neutralized by Na_2CO_3 (1.0 mmol). Then, the reaction was cool to room temperature and then the collected precipitates were washed by cold methanol (**Scheme-I**). The obtained products were soluble in organic solvents such as DMSO, CH_3OH and CH_2Cl_2.

[Zn(II)(BHB)$_2$]: White solid, yield: 93.0%; ESI-MS: 574.3 [M + H] (calcd. 576.8). FTIR (KBr, ν_{max}, cm^{-1}): 3151 (N–H), 3021 (C–H), 1597 (C=N), 1560 (C=C), 1475, 1387, 1279 (C–O), 1179, 1074 (N–N), 882, 837, 756 (C–H), 664, 592, 470 (Zn–N), 423 (Zn–O). ^{1}H NMR (600 MHz, DMSO-d_6, δ ppm): 9.73 (1H, OH); 8.55 (1H, CH=N); 7.95 (d, *J* = 5.5, 2H, Bz), 7.24 (1H, Sal); 7.15 (1H, Sal.); 6.80 (d, *J* = 6.0, 2H, Bz), 6.59 (1H, Sal). UV-Vis [MeOH, 3.0×10^{-5} M, λ (nm), ε (cm^{-1} M^{-1})]: 220 (18,667), 257 (11,267), 300 (18,933), 378 (11,100).

[Zn(II)(CBHB)$_2$]: Yellowish solid, yield: 95.0%. ESI-MS: 678.5 [M + Cl^-] (calcd. 680.2). FTIR (KBr, ν_{max}, cm^{-1}): 3169 (N–H), 3021 (C–H), 1594 (C=N), 1557 (C=C), 1472, 1364 (N=N), 1291 (C–O), 1175, 1121 (N–N), 942, 833, 725 (C–H), 653, 549 (Zn–N), 470 (Zn–O); ^{1}H NMR (600 MHz, DMSO-d_6, δ ppm): 9.68 (1H, OH); 8.48 (1H, CH=N); 7.92 (d, *J* = 6.0, 2H, Bz), 7.24 (1H, Sal); 7.05 (1H, Sal); 6.77 (d, *J* = 7.0, 2H, Bz); UV-Vis [MeOH, 3.0×10^{-5} M, λ (nm), ε (cm^{-1} M^{-1})]: 220 (20,833), 260 (12,933), 302 (22,967), 362 (10,767).

[Zn(II)(MBHB)$_2$]: Yellowish solid, yield: 91.0%. ESI-MS: 671.0 [M + Cl^-] (calcd. 671.3). FTIR (KBr, ν_{max}, cm^{-1}): 3185 (N–H), 3031 (C–H), 1595 (C=N), 1505 (C=C), 1446, 1385 (N=N), 1287 (C–O), 1214, 1172, 1075 (N–N), 971, 846, 738 (C–H), 666, 485 (Zn–N), 444 (Zn–O); ^{1}H NMR (600 MHz, DMSO-d_6, δ ppm): 9.61 (1H, OH); 8.45 (1H, CH=N); 7.88 (d, *J* = 7.0, 2H, Bz), 6.77 (d, *J* = 6.5, 1H, Sal); 6.73 (d, *J* = 7.5, 2H, Bz), 6.71 (d, *J* = 6.5, 1H, Sal), 6.35 (1H, Sal), 3.69 (3H, OCH_3); UV-Vis [MeOH, 3.0×10^{-5} M, λ (nm), ε (cm^{-1} M^{-1})]: 232 (20,967), 324 (19,933), 390 (16,233).

[Zn(II)(MBIB)$_2$]: Yellow solid, yield: 993.5 %). ESI-MS: 640.8 [M + Cl^-] (calcd. 641.3). FTIR (KBr, ν_{max}, cm^{-1}): 3400 (H_2O), 3165 (N–N), 3054 (C–H), 1600 (C=N), 1533 (C=C), 1446, 1374 (N=N), 1212 (C–O), 1110 (N–N), 1028, 973, 856, 734, 713 (C–H), 542 (Zn–N), 464 (Zn–O); ^{1}H NMR (600 MHz, DMSO-d_6, δ ppm): 8.59 (1H, CH=N); 8.67 (2H, Bz), 7.97 (d, *J* = 4.0, 2H, Bz), 6.85 (d, *J* = 6.5, 1H, Sal.); 6.79 (d, *J* = 6.0, 1H, Sal), 6.40 (t, *J* = 6.0, 1H, Sal), 3.73 (3H, OCH_3); UV-Vis [MeOH, 3.0×10^{-5} M, λ (nm), ε (cm^{-1} M^{-1})]: 234 (18,733), 330 (13,533), 402 (11,700).

Luminescent properties: Luminescent analysis of the synthesized zinc(II) complexes in dichloromethane at 5×10^{-5} M were studied by photoluminescence spectroscopy using a Horiba Fluorolog spectrofluorometer.

***In vitro* α-glucosidase inhibition assay:** *p*-Nitrophenyl α-D-glucopyranoside (PNPG) method was used to determine α-glucosidase activity and inhibitor screening [46,47]. PNPG can be hydrolyzed to the yellow product *p*-nitrophenol (PNP) under the influence of α-glucosidase. Tested samples were diluted by DMSO and deionized water into the solutions of various concentrations. Acarbose was used as the standard inhibitor. The enzymatic reaction mixture composed of α-glucosidase (0.2 U/mL), PNPG (2.5 mM), tested compound (10 µL) and potassium phosphate buffer (0.1 M, pH 6.8) was incubated at 37 ºC for 30 min. After incubation time, the reaction was stopped by Na_2CO_3 solution (0.1 M). The absorbance of yellow colour induced by the formation of PNP was identified using a BIOTEK machine at 410 nm. All the experiments were conducted in triplicates. The α-glucosidase inhibition activity of testing samples was determined as the following equation:

$$\text{Inhibition (\%)} = \frac{A_r - A_s}{A_r} \times 100$$

where A_r is the absorbance of negative reference (water) and A_s is the absorbance of samples. The IC_{50} (concentration which induces the inhibition of 50% α-glucosidase activity) was calculated using Table curve software.

RESULTS AND DISCUSSION

The aromatic hydrazones were synthesized by condensing aromatic aldehydes with 4-hydroxybenzohydrazide or isonicotinohydrazide in ethanol to afford the good reaction yields up to 86.5%. Then, the obtained hydrazone ligands can coordinate with $Zn(CH_3COO)_2{\cdot}2H_2O$ in the molecular rate of 2:1 to synthesize zin(II) complexes in methanol in the high coordination yields (91.0-95.0%).

The HRMS spectra of received aromatic hydrazones showed the pseudo-molecular ion signals as $[M+H]^+$ which are consistent with the molecular weights of the synthesized ligands. On the ESI-MS spectra of synthesized zinc(II) complexes, the

pseudo-molecular ion signals were appeared as $[M+H]^+$ or $[M+Cl]^-$ which are well suitable to the above formulae in the ratio 1:2 of Zn(II) and aromatic hydrazone ligand proportionally.

FTIR spectra of the synthesized ligands express typical signals at 3348-3202 cm^{-1} and 3231-3150 cm^{-1} for O–H and N–H stretching vibrations, respectively. The characteristic peaks at 1688-1616 cm^{-1} and 1607-1603 cm^{-1} belong to the stretching vibrations of C=O and C=N, respectively. The observed signals at 1286-1267 cm^{-1} and 1114-1066 cm^{-1} may correspond to stretching frequencies of C–O and N–N, respectively. In FTIR spectra of zinc(II) complexes, some shifts in the peaks of the obtained aromatic hydrazones are observed. The O–H stretching vibrations were disappeared while the N–H stretching vibrations of phenyl rings were still observed at 3185-3151 cm^{-1} which has proved that the OH groups were impacted in coordination to form the zinc(II) complexes [48,49]. New signals at 549-470 cm^{-1} and 470-423 cm^{-1} are assigned respectively to new formed Zn–N and Zn–O bondings, which demonstrate the formation of aromatic hydrazone zinc(II) complexes.

^{1}H NMR spectra of obtained hydrazone ligands show all signals for protons of functional groups such as the protons of NH and OH (Sal) appeared at 12.25-11.87 ppm and 11.42-10.71 ppm, respectively as single peaks. Similarly, the protons at 10.18-10.16 ppm and 8.71-8.58 ppm as single peaks are due to the of OH(Ph) and azomethine CH=N. At last, the protons of aromatic rings and methoxy appeared at 8.79-6.86 ppm and 3.82-3.81 ppm, respectively. In ^{13}C NMR spectra of the synthesized hydrazone ligands, the signals are observed at 162.54-161.27 ppm for the carbons of C=O; at 160.94-160.84 ppm for the carbons of C–OH (Ph); at 157.40-147.94 ppm for carbons of C–OH (Sal); at 147.62-145.23 ppm for the carbons of azomethine C=N; at 139.98-113.79 ppm for other aromatic carbons probably. In addition, the typical signals at 122.87 ppm for the carbon of C–Cl of **CBHB**; at 147.95, 55.86 ppm and 147.59, 55.82 ppm for the carbons of C–OCH_3 of **MBHM** and **MBIB** ligands, respectively are observed. The characteristic signal for two carbons of C=N–C of **MBIB** were found at 150.33 ppm. In ^{1}H NMR spectra of zinc(II) complexes, the characteristic signals were appeared at 9.73-9.61 ppm for the protons of OHs (Ph); at 8.59-8.45 ppm for the protons of azomethine CH=Ns. The phenyl protons of **[Zn(II)(BHB)$_2$]**, **[Zn(II)(CBHB)$_2$]** and **[Zn(II)(MBHB)$_2$]** were found usually as two double peaks at 7.95-7.88 ppm and 6.80-6.73 ppm while the protons of pyridyl protons of **[Zn(II)(BHB)$_2$]** were observed at 8.67 and 7.97 ppm. Herein, The absence of the characteristic signals of OHs (Sal) has definitely confirmed their role in the formation of zinc(II) complexes. The coordination of the aromatic hydrazone ligands have induced the weakness of proton peaks of NH and salicyl protons. However, in some cases, these signals are not observed clearly.

The electronic absorption spectra of hydrazone ligands and their zinc(II) complexes were measured in methanol from 200 to 800 nm at room temperature. In the free ligands, the electronic absorption maxima were observed at 224-225 nm attributed to $\pi\rightarrow\pi^*$ transition of aromatic rings, at 292-310 and 340-393 nm assigned to $n\rightarrow\pi^*$ transition of lone pair of electrons of heteroatoms probably (Fig. 1). In the zinc(II) complexes, the main electronic absorption peaks were established at 220-234 nm consistent with $\pi\rightarrow\pi^*$ transition of aromatic rings and at 300-330 nm and 362-402 nm assignable to $n\rightarrow\pi^*$ transition of lone pair of electrons of heteroatoms (Fig. 2). The observed absorption maxima of the received hydrazone complexes are shifted toward longer wavelengths compared with the absorption peaks of the synthesized ligands [49,50]. These results have proved the coordination of Zn(II) with the aromatic hydrazone ligands. All the synthesized zinc(II) complexes are diamagnetic and in octahedral coordination geometry around the central ion Zn^{2+} [51,52].

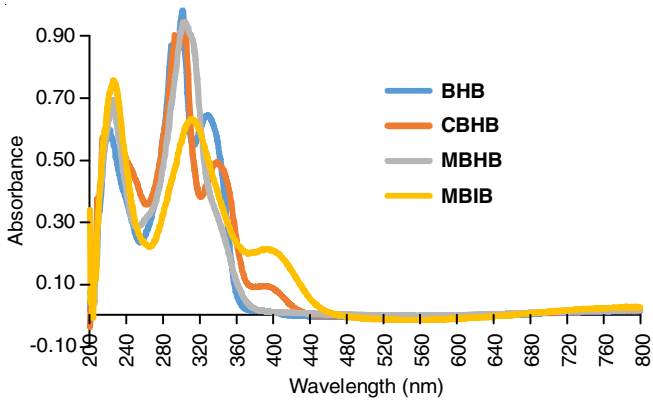

Fig. 1. The UV-visible spectra of synthesized aromatic hydrazone ligands

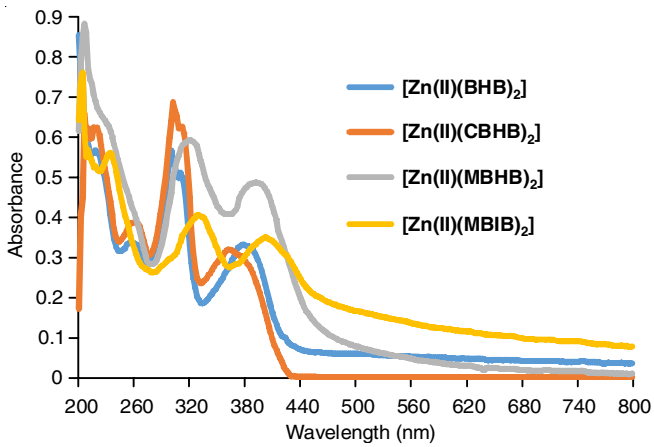

Fig. 2. The UV-visible spectra of aromatic hydrazone zinc(II) complexes of hydrazones

Fluorescent spectra: Fluorescent spectra of the synthesized zinc(II) complexes were recorded in dichloromethane are shown in Fig. 3. Upon complexation of the hydrazones containing π-conjugation system with Zn^{2+}, the emission peak is usually blue shifted with an increasing fluorescence intensity [53]. In this case, the emission signal of **[Zn(II)(BHB)$_2$]** was found at 466 nm with high intensity. The different substituents of salicyl ring induce the emission wavelengths of the **[Zn(II)(CBHN)$_2$]** and **[Zn(II)(MBHB)$_2$]** to be more blue shifted at 495 and 503 nm, respectively with the lower intensities due to the localized π-electrons [54]. The *p*-pyridyl ring of **MBIB** also offer a longer wavelength for the luminescent maximum of **[Zn(II)(MBIB)$_2$]** observed at 552 nm.

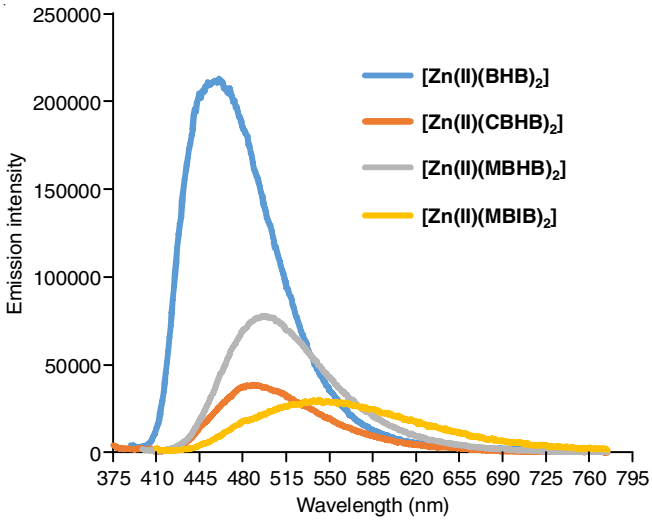

Fig. 3. The emission spectra of the prepared aromatic hydrazone zinc(II) complexes

Antidiabetic activity: The ability of the free ligands and its Zn(II) complexes for antidiabetic activity as α-glucosidase inhibition was evaluated. α-Glucosidase inhibitors can limit the conversion of disaccharides to monosaccharides and induces the delay of carbohydrate digestion. Hence, the α-glucosidase inhibitors can reduce hyperglycemia and control the diabetes [40,41]. The experimental results showed that hydrazone ligands exhibit the weak activity with IC_{50} > 128 µg/mL, when its Zn(II) complexes express the stronger activity with IC_{50} < 105 µg/mL. The substituted groups perform an efficient influence to the antidiabetic activity of the synthesized zinc(II) complexes. The electron withdrawing chloride seems to induce the weaker antidiabetic activity while the electron donoring groups of methoxy can enhance the α-glucosidase inhibition (Table-1). Especially, **[Zn(II)(MBHB)$_2$]** has showed the best antidiabetic activity with IC_{50} = 0.49 µg/mL, which is much stronger than the standard drug acarbose with IC_{50} = 147.86 µg/mL.

TABLE-1
INHIBITORY ACTIVITY OF AROMATIC HYDRAZONES AND THEIR ZINC(II) COMPLEXES AGAINST α-GLUCOSIDASE

Tested compounds	IC_{50} (µg/mL)
BHB	> 128
CBHB	> 128
MBHB	> 128
MBIB	> 128
[Zn(II)(BHB)$_2$]	3.74 ± 0.27
[Zn(II)(CBHB)$_2$]	103.49 ± 8.65
[Zn(II)(MBHB)$_2$]	0.49 ± 0.02
[Zn(II)(MBIB)$_2$]	6.00 ± 0.57
Acarbose	147.86 ± 4.69

Conclusion

In this study, zinc(II) complexes containing some aromatic hydrazones were synthesized. Based on various spectral investigations, the molecular ratio 1:2 of zinc(II) and the hydrazone ligand was offered. The ligands coordinated with the metal ion *via* the carbonyl oxygen and deprotonated oxygen of salicyl ring in the tetrahedral geometry. The fluorescent spectra have showed that the high intensity and blue shifted emission peak in the [Zn(II)(BHB)$_2$] complex. The zinc(II) complexes containing the aromatic hydrazone ligands with different substituted groups possess the emission maxima of the longer wavelengths. The α-glucosidase inhibition of the synthesized Zn(II) complexes are much better than the inhibition of the aromatic hydrazone ligands. Among the synthesized zn(II) complexes, [Zn(II)(MBHB)$_2$] complex has expressed the best antidiabetic activity with IC_{50} = 0.49 µg/mL much stronger than acarbose, a standard drug, with IC_{50} = 147.86 µg/mL.

ACKNOWLEDGEMENTS

The authors express their sincere gratitude to Vietnam Academy of Science and Technology for the financial support by Project No. CSCL06.06/22-23.

CONFLICT OF INTEREST

The authors declare that there is no conflict of interests regarding the publication of this article.

REFERENCES

1. P.C. Sharma, D. Sharma, A. Sharma, N. Saini, R. Goyal, M. Ola, R. Chawla and V.K. Thakur, *Mater. Today Chem.*, **18**, 100349 (2020); https://doi.org/10.1016/j.mtchem.2020.100349
2. A.-M. Stadler and J. Harrowûeld, *Inorg. Chim. Acta*, **362**, 4298 (2009); https://doi.org/10.1016/j.ica.2009.05.062
3. H. Kargar, M. Fallah-Mehrjardi and K.S. Munawar, *Coord. Chem. Rev.*, **501**, 215587 (2024); https://doi.org/10.1016/j.ccr.2023.215587
4. O.M.I. Adly and A. Taha, *J. Mol. Struct.*, **1038**, 250 (2013); https://doi.org/10.1016/j.molstruc.2013.01.035
5. P. Yang, H. Chen, Z.-Z. Wang, L.-L. Zhang, D.-D. Zhang, Q.-S. Shi and X.-B. Xie, *J. Inorg. Biochem.*, **213**, 111248 (2020); https://doi.org/10.1016/j.jinorgbio.2020.111248
6. M.K. Hossain, M. Haukka, G.C. Lisensky, M.G. Richmond and E. Nordlander, *Polyhedron*, **258**, 117020 (2024); https://doi.org/10.1016/j.poly.2024.117020
7. M. Fallah-Mehrjardi, H. Kargar and K.S. Munawar, *Inorg. Chim. Acta*, **560**, 121835 (2024); https://doi.org/10.1016/j.ica.2023.121835
8. S.D. Kurbah, M. Asthana, I. Syiemlieh and R.A. Lal, *Curr. Organocatal.*, **4**, 189 (2018); https://doi.org/10.2174/2213337205666180124161832
9. C. Shalini, M. Akilesh, G. Sathiyaraj, N.S.P. Bhuvanesh, K.S. Neethu, M.V. Kaveri and N. Dharmaraj, *Appl. Organomet. Chem.*, **38**, e7709 (2024); https://doi.org/10.1002/aoc.7709
10. H.A. El-Ghamry, M. Gaber, F.M. Alkhatib, H.F. Al Shareef, K.M. Takroni and S.K. Fathalla, *RSC Adv.*, **14**, 30673 (2024); https://doi.org/10.1039/D4RA05769D
11. A. Ciupa, *RSC Adv.*, **15**, 3465 (2025); https://doi.org/10.1039/D4RA09068C
12. S.A. Rupa, A.M.P. Md, W.E. Ghann and A. Abdullahi, *RSC Adv.*, **13**, 23819 (2023); https://doi.org/10.1039/D3RA04364A
13. Z.-H. Zhang, Y.-M. Zhang, X.-T. Kan, Q.-Y. Yang, Y.-J. Li, T.-B. Wei, H. Yao and Q. Lin, *Dyes Pigments*, **191**, 109389 (2021); https://doi.org/10.1016/j.dyepig.2021.109389
14. Y. Zhang, Q. Li, Q. Zhang, Q. Lin, C. Cao, M. Liu and T. Wei, *Chin. J. Chem.*, **29**, 1529 (2011); https://doi.org/10.1002/cjoc.201180275
15. M. Saravanan and S. Abraham Rajasekar, *Opt. Mater.*, **54**, 217 (2016); https://doi.org/10.1016/j.optmat.2016.02.039
16. T.A. Khattab, *Mater. Chem. Phys.*, **254**, 123456 (2020); https://doi.org/10.1016/j.matchemphys.2020.123456

17. R.M. Snari, M. Alsahag, A. Alisaac, A. Bayazeed, A. Alsoliemy, M.E. Khalifa and N.M. El-Metwaly, *J. Mol. Liq.*, **366**, 120149 (2022); https://doi.org/10.1016/j.molliq.2022.120149
18. P. Popczyk, A. Ghinet, C. Bortolus, L. Kamus, M.F. Lensink, J. de Ruyck, B. Sendid and F. Dubar, *J. Enzyme Inhib. Med. Chem.*, **39**, 2429109 (2024); https://doi.org/10.1080/14756366.2024.2429109
19. M.S. Alam, S.-U. Choi and D.-U. Lee, *Bioorg. Med. Chem.*, **25**, 389 (2016); https://doi.org/10.1016/j.bmc.2016.11.005
20. L. Popiolek, A. Biernasiuk, A. Berecka, A. Gumieniczek, A. Malm and M. Wujec, *Chem. Biol. Drug Des.*, **91**, 915 (2018); https://doi.org/10.1111/cbdd.13158
21. S. Emami, M. Valipour, F.K. Komishani, F. Sadati-Ashrafi, M. Rasoulian, M. Ghasemian, M. Tajbakhsh, P.H. Masihi, A. Shakiba, H. Irannejad and N. Ahangar, *Bioorg. Chem.*, **112**, 104943 (2021); https://doi.org/10.1016/j.bioorg.2021.104943
22. N. Agrawal, R. Mishra, S. Pathak, A. Goyal and K. Shah, *Lett. Org. Chem.*, **20**, 123 (2023); https://doi.org/10.2174/1570178619666220831122614
23. B.R. Thorat, S.N. Mali, D. Rani and R.S. Yamgar, *Curr. Computeraided Drug Des.*, **17**, 294 (2021); https://doi.org/10.2174/1573409916666200302120942
24. H. Ünver, B. Berber, R. Demirel and A.T. Koparal, *Anticancer. Agents Med. Chem.*, **19**, 1658 (2019); https://doi.org/10.2174/1871520619666190318125824
25. M. Yousaf, M. Khan, M. Ali, W.A. Shams, M. Ali, *Curr. Bioact. Compd.*, **18**, e190422203781 (2022); https://doi.org/10.2174/1573407218666220419105140
26. J. Zhao, Y. Wang, W. Chen, G. Hao, J. Sun, Q. Shi, F. Tian and R. Ma, *RSC Adv.*, **12**, 3073 (2022); https://doi.org/10.1039/D1RA08616B
27. Z. Moussa, M. Al-Mamary, S. Al-Juhani and S.A. Ahmed, *Heliyon*, **6**, e05019 (2020); https://doi.org/10.1016/j.heliyon.2020.e05019
28. Ü.Ö. Özdemir, N. Akkaya and N. Özbek, *Inorg. Chim. Acta*, **400**, 13 (2013); https://doi.org/10.1016/j.ica.2013.01.031
29. T. Benkovic, A. Kendel, J. Parlov-Vukovic, D. Kontrec, V. Chis, S. Miljanic and N. Galic, *Spectrochim. Acta A Mol. Biomol. Spectrosc.*, **190**, 259 (2018); https://doi.org/10.1016/j.saa.2017.09.038
30. X. Wang, S.-W. Yan, J. Yang, D.-R. Xiao, H.-Y. Zhang, J.-L. Zhang, X.-L. Chi and E.-B. Wang, *Inorg. Chim. Acta*, **409**, 208 (2014); https://doi.org/10.1016/j.ica.2013.09.031
31. L. Rochette, M. Zeller, Y. Cottin and C. Vergely, *Biochim. Biophys. Acta, Gen. Subj.*, **1840**, 2709 (2014); https://doi.org/10.1016/j.bbagen.2014.05.017
32. F.M. Ashcroft and P. Rorsman, *Cell*, **148**, 1160 (2012); https://doi.org/10.1016/j.cell.2012.02.010
33. C.-H. Chang, Y.-D. Jiang, C.-H. Chung, L.-T. Ho and L.-M. Chuang, *J. Formos. Med. Assoc.*, **111**, 617 (2012); https://doi.org/10.1016/j.jfma.2012.09.009
34. M. Dhameja and P. Gupta, *Eur. J. Med. Chem.*, **176**, 343 (2019); https://doi.org/10.1016/j.ejmech.2019.04.025
35. U. Ghani, *Eur. J. Med. Chem.*, **103**, 133 (2015); https://doi.org/10.1016/j.ejmech.2015.08.043
36. S. Malik, M.A. Lodhi, S. Ayaz and Z. Ullah, *J. Mol. Liq.*, **400**, 124572 (2024); https://doi.org/10.1016/j.molliq.2024.124572
37. C.I. Chukwumaa, S.S. Mashelea, K.C. Ezeb, G.R. Matowanea and S. Md, *Pharmacol. Res.*, **155**, 104744 (2020); https://doi.org/10.1016/j.phrs.2020.104744
38. M. Huseynovaa, A. Medjidov, P. Taslimi and M. Aliyeva, *Bioorg. Chem.*, **83**, 55 (2019); https://doi.org/10.1016/j.bioorg.2018.10.012
39. Y. Yoshikawa and H. Yasui, *Curr. Top. Med. Chem.*, **12**, 210 (2012); https://doi.org/10.2174/156802612799078874
40. G.M. Esteban-Parra, E. San Sebastián, J. Cepeda, C. Sánchez-González, L. Rivas-García, J. Llopis, P. Aranda, M. Sánchez-Moreno, M. Quirós and A. Rodríguez-Diéguez, *J. Inorg. Biochem.*, **212**, 111235 (2020); https://doi.org/10.1016/j.jinorgbio.2020.111235
41. M. Demurtas, A. Baldisserotto, I. Lampronti, D. Moi, G. Balboni, S. Pacifico, S. Vertuani, S. Manfredini and V. Onnis, *Bioorg. Chem.*, **85**, 568 (2019); https://doi.org/10.1016/j.bioorg.2019.02.007
42. C.B. Juliana de Oliveira, C.C.F. Tanos, S.R. LaPlante and D.F.V. José, *Mini Rev. Med. Chem.*, **20**, 342 (2020); https://doi.org/10.2174/1389557519666191014142448
43. A.M. John, J. Jose, R. Thomas, K.J. Thomas and S.P. Balakrishnan, *Spectrochim. Acta Part A: Mol. Biomol. Spect.*, **236**, 118329 (2020); https://doi.org/10.1016/j.saa.2020.118329
44. M.C. Mandewale, B. Thorat, Y. Nivid, R. Jadhav, A. Nagarsekar and R. Yamgar, *J. Saudi Chem. Soc.*, **22**, 218 (2018); https://doi.org/10.1016/j.jscs.2016.04.003
45. B. Kumar, J. Devi, A. Dubey, A. Tufail and B. Taxak, *Sci. Rep.*, **13**, 15906 (2023); https://doi.org/10.1038/s41598-023-42180-4
46. E.N. Agbo, *Res. Chem.*, **14**, 102102 (2025); https://doi.org/10.1016/j.rechem.2025.102102
47. D. Avci, S. Altürk, F. Sönmez, Ö. Tamer, A. Basoglu, Y. Atalay, B.Z. Kurt and N. Dege, *J. Mol. Struct.*, **1197**, 645 (2019); https://doi.org/10.1016/j.molstruc.2019.07.039
48. E. Pahontu, D.-C. Ilies, S. Shova, C. Oprean, V. Pãunescu, O.T. Olaru, F.S. Rãdulescu, A. Gulea, T. Rosu and D. Drãgãnescu, *Molecules*, **22**, 650 (2017); https://doi.org/10.3390/molecules22040650
49. M.C. Mandewale, B. Thorat, D. Shelke and R. Yamgar, *Bioinorg. Chem. Appl.*, **2015**, 153015 (2015); https://doi.org/10.1155/2015/153015
50. M.C. Mandewale, S. Kokate, B. Thorat, S. Sawant and R. Yamgar, *Arab. J. Chem.*, **12**, 4479 (2016); https://doi.org/10.1016/j.arabjc.2016.07.016
51. L. Li, Y.Z. Zhang, E. Liu, C. Yang, J.A. Golen, A.L. Rheingold and G. Zhang, *J. Mol. Struct.*, **1110**, 180 (2016); https://doi.org/10.1016/j.molstruc.2016.01.051
52. S. Aslkhademi, N. Noshiranzadeh, M.S. Sadjadi, K. Mehrani and N. Farhadyar, *Polyhedron*, **160**, 115 (2019); https://doi.org/10.1016/j.poly.2018.12.023
53. M.C. Mandewale, S. Kokate, B. Thorat, S. Sawant and R. Yamgar, *Arab. J. Chem.*, **12**, 4479 (2019); https://doi.org/10.1016/j.arabjc.2016.07.016
54. N. Sunitha, C.I.S. Raj and B.S. Kumari, *Res. Chem.*, **4**, 100588 (2022); https://doi.org/10.1016/j.rechem.2022.100588